Tuesday December 3, 2013

- Don't forget to evaluate this course online after final
- Seth Dee talk at 2pm
- Slow Slip Events and Rate/State Friction (micro lecture), Japan, Taiwan, San Andreas, Cascadia, Central America, Mexico, New Zealand, Caribbean
- Work on Problem Set #5
- Work on Projects

Slow Slip Event on San Andreas Fault

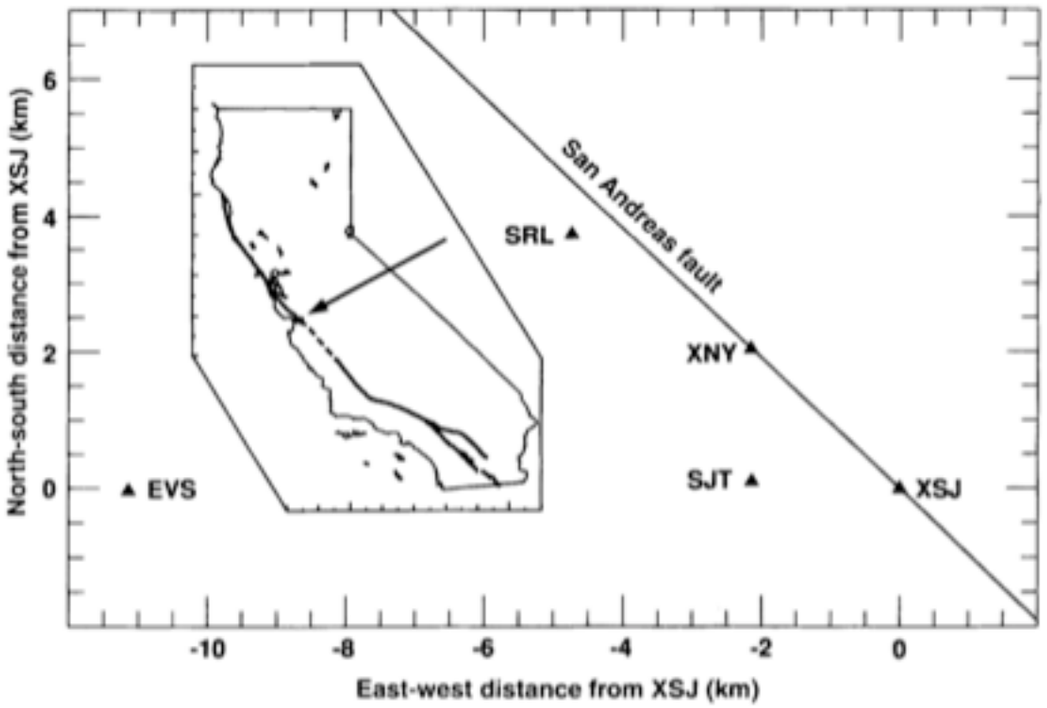

FIG. 1 Map of the location of borehole instruments SRL, SJT and EVS; of creepmeters XSJ and XNY, and of the San Andreas fault. The insert of California (large tick marks are for 1 degree of latitude and longitude) shows the site area (indicated by the arrow) and the main trace (heavy line) of the San Andreas fault. The dashed section south of the study area indicates the creeping part of the fault. Creepmeters span the fault and measure the relative displacement across it. Borehole strainmeters are located off the fault both to avoid installation in fault zone material and to allow sensitivity to deformation at depth on the fault.

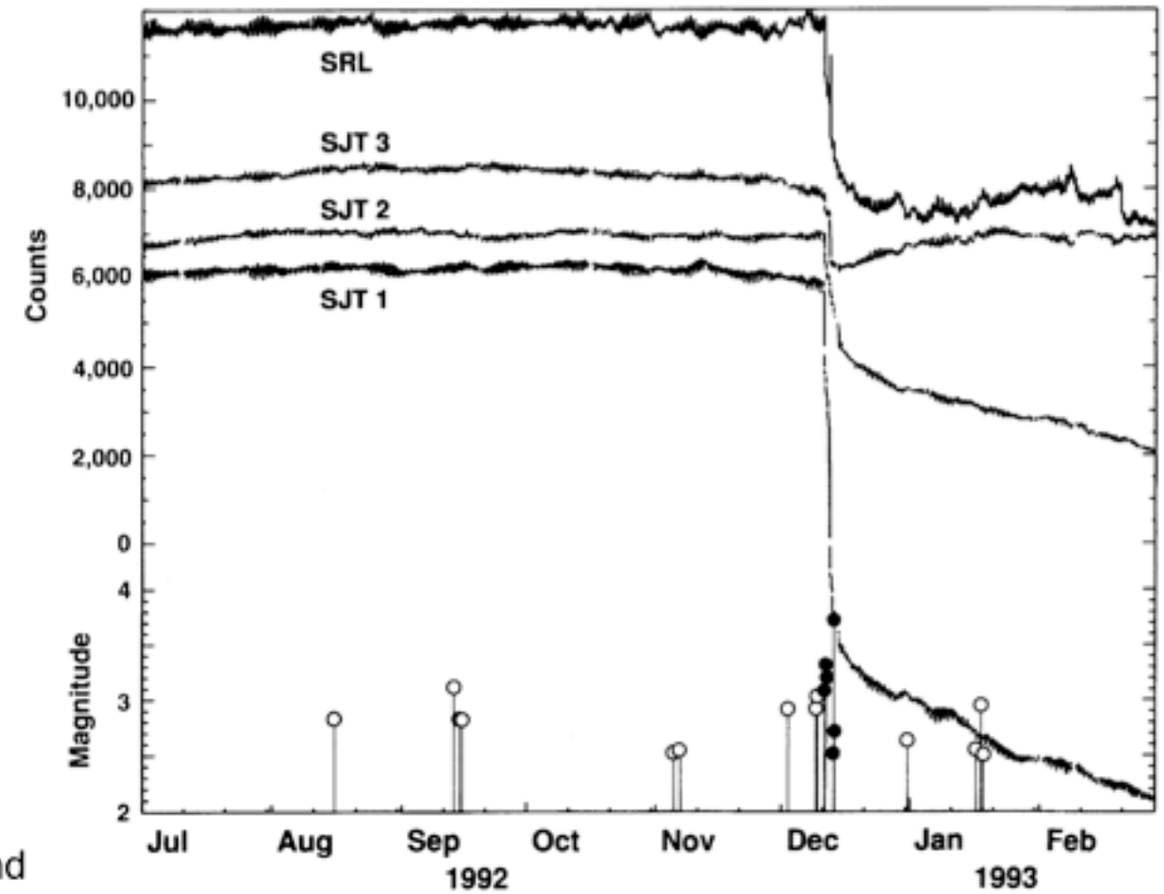

Linde et al., 1996, *Nature*

see class page for .pdf

Slow Slip Event on San Andreas Fault

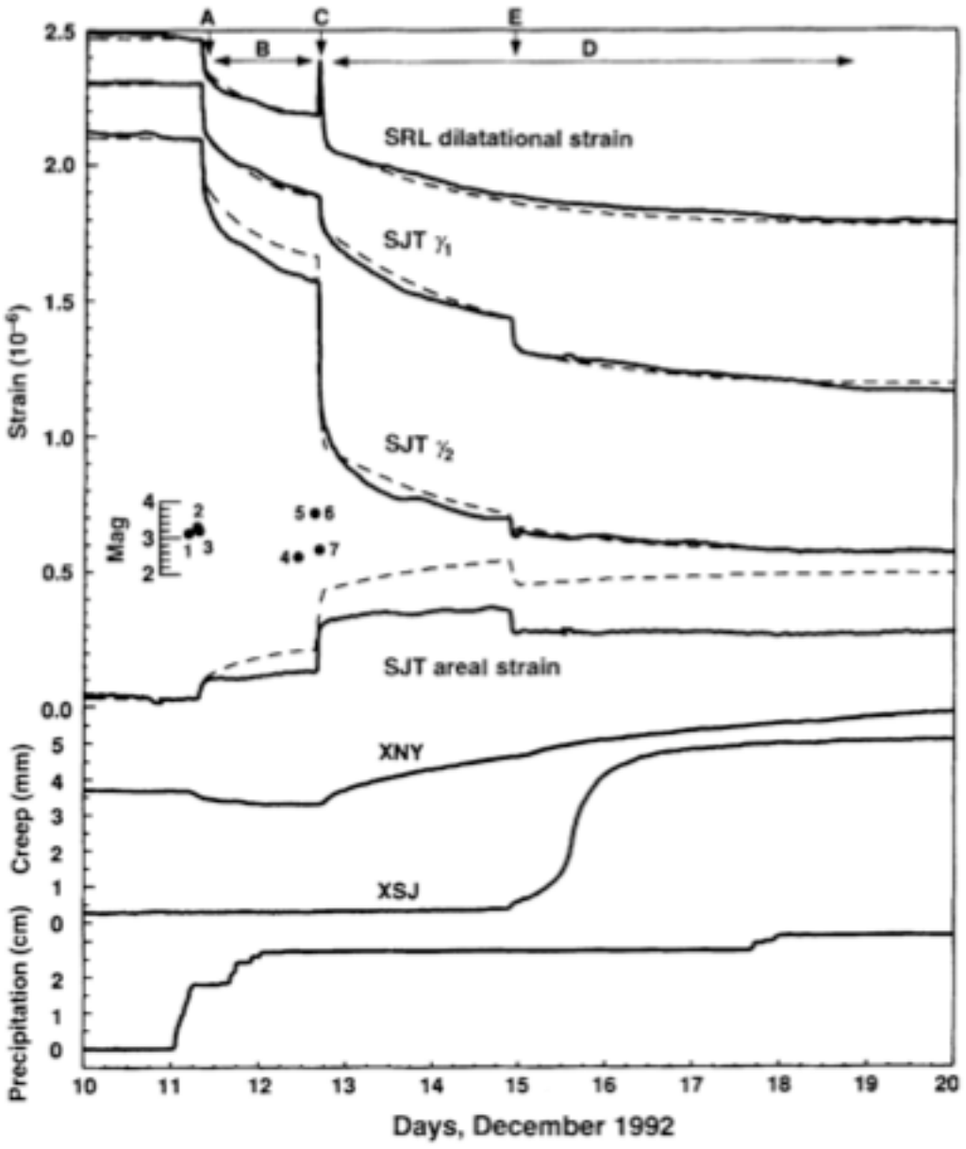

FIG. 3 Strain data (solid lines) from SRL and SJT for 10 days in December 1992 covering the duration of coherent slow changes. SRL records dilatational strain. From SJT we get γ_1 shear at N45 W (approximately fault-parallel) fault-normal shear γ_2, and areal strain. Earth tides and strain changes induced by atmospheric pressure have been removed; some residual tidal variations remain, including small changes before the initiation of the slow sequence. Creep data (XNY and XSJ) and precipitation are also shown. Earthquake times and magnitudes are shown in the insert numbered in order of origin time; there are two m_L 3.7 events on 12 December. The labels A–E indicate slow events within the sequence. Dashed curves are results from model calculations. Calculated coseismic changes are included but are not significant. The results are not significantly affected by reasonable errors in the site locations or by the non-verticality of the fault. The fit to SRL dilatation and to γ_1 shear is essentially perfect. We could improve the fit to areal strain by changing the amount of slip on X and Y (see text and Fig. 4) for events A, B and D without decreasing the fit to dilatation and γ_1, but the quality of the fit for γ_2 would decrease. This apparent discrepancy may be a result of using a homogenous Earth model in processing the data from the three sensors of SJT to produce the areal and shear strains. Preliminary finite-element modelling of the differences in material elastic constants on opposite sides of the fault indicates that area strain has been underestimated and that γ_2 has been overestimated.

Linde et al., 1996, *Nature*

see class page for .pdf

Slow Slip Event on San Andreas Fault

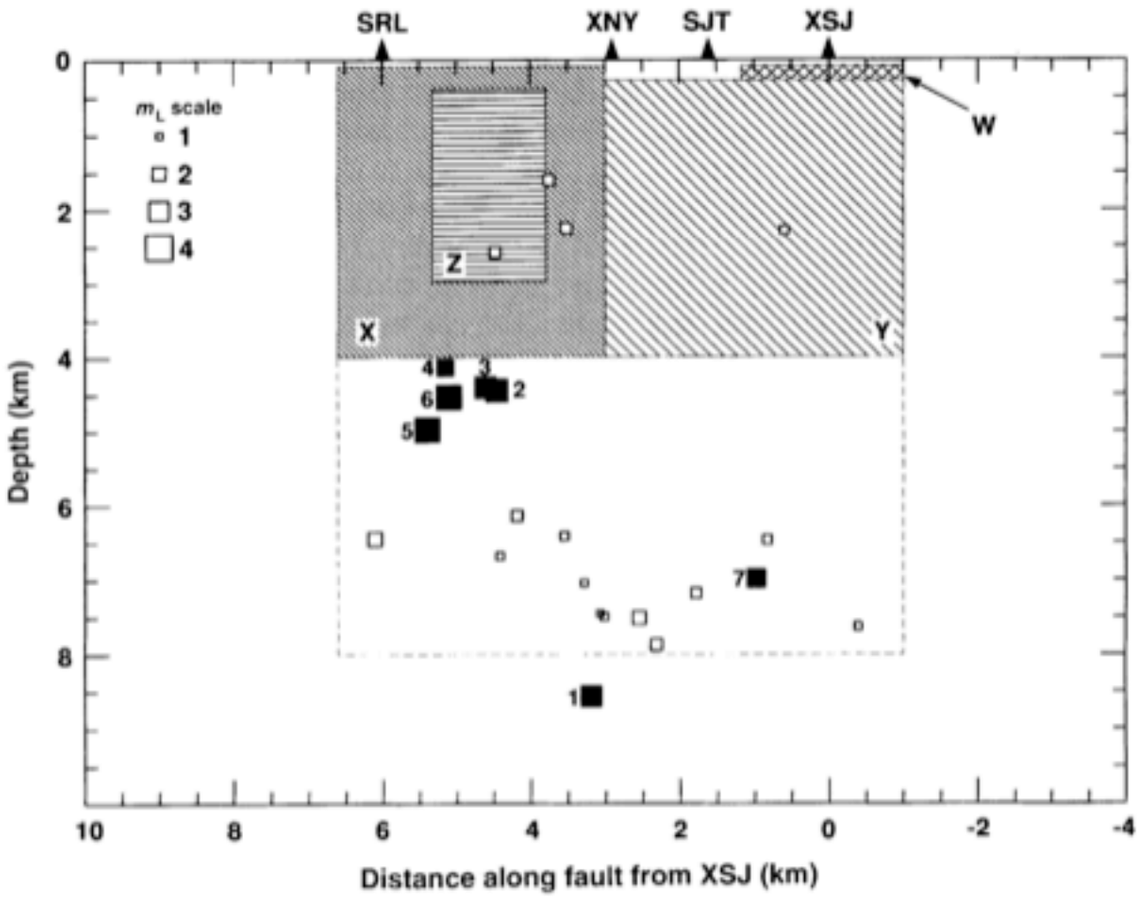

FIG. 4 Vertical section in the local strike direction of the San Andreas fault. Earthquakes are shown as filled squares for events with magnitudes $\geqslant 2.5$ (numbered as in Fig. 3), and open squares for smaller events; areas of these events are much smaller than for the slow slip. XSJ and XNY show the locations of creepmeters; SRL and SJT sites are shown projected onto the fault. Shaded areas are those used for the model calculations. Aseismic slip in X and Y corresponds to strain events A, B and D. Aseismic slip on Z and W corresponds to events C and D respectively. Dashed lines indicate that the source depths for X and Y could extend to 8 km.

Linde et al., 1996, *Nature*

see class page for .pdf

Slow Slip Events in the Laboratory

Fig. 1. A full experiment showing repetitive, slow stick-slip. (**A**) Shear stress (τ; top solid line) during repeating stick-slip failure of serpentinite gouge under constant far-field velocity (dashed line). Like earthquake cycles, τ builds over long periods but is released in punctuated slip events, creating steps in fault slip displacement. (Inset) The double-direct shear arrangement with the piezo-electric transducers (PZT). (**B**) Subplots show 30-s windows for each stick-slip event in (A), with event durations from 1 to 30 s. Fault slip (gray lines) is driven by stress release (black lines). There is a clear progression from small impulsive events to large slow events with increasing net displacement.

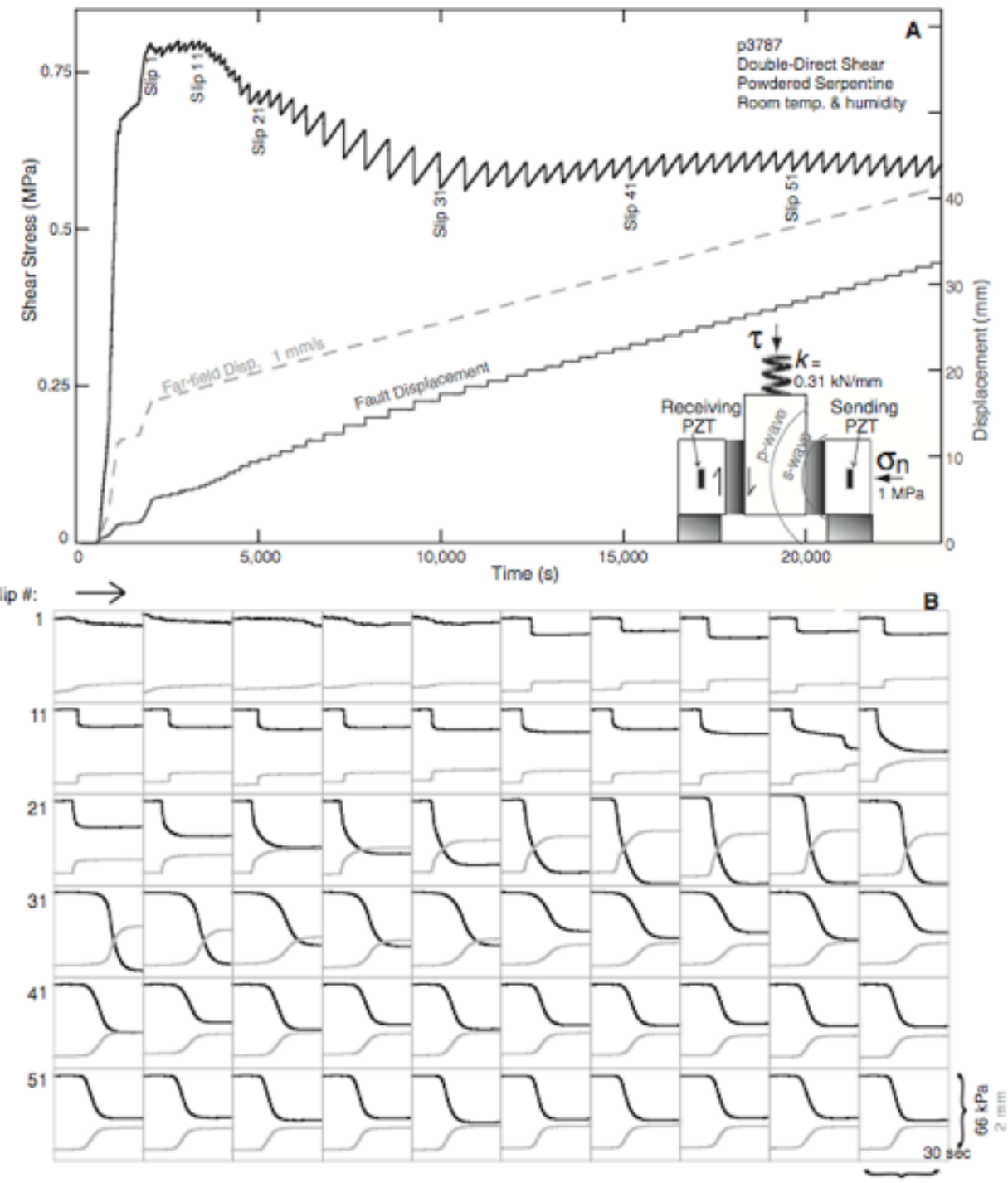

Kaproth and Marone, 2013, *Science*

Slow Slip Events from *Rate and State* Friction

The classic demonstration of how friction physics explains earthquakes

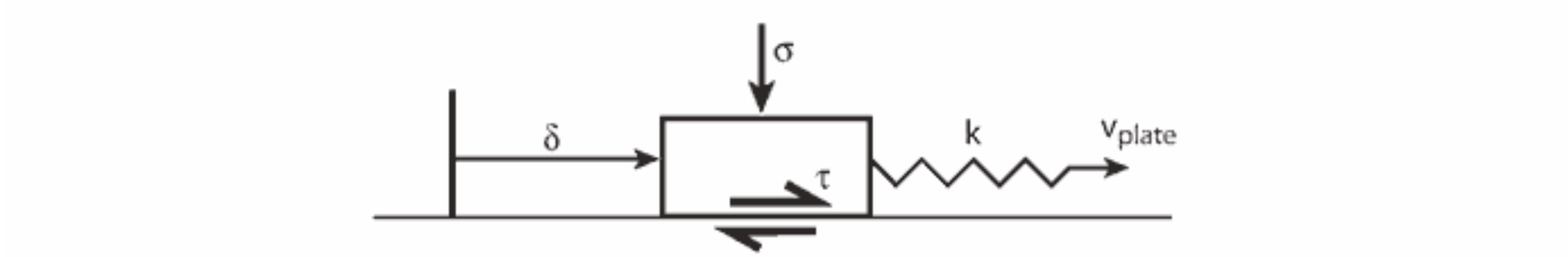

Figure 11.1. Single degree of freedom spring-slider system. A block is pressed against a flat interface with normal stress σ. Frictional resistance to slip is τ. A spring with stiffness k is attached to the block, the far end of which displaces at constant rate v_{plate}. The cumulative displacement of the block is δ.

$$\tau = f\sigma$$

- dynamic (moving) vs. static (not moving) friction
  - pull slow "stable sliding", pull fast "stick-slip"

See Segall, "Earthquake and Volcano Deformation" Chapter 11.3

Slow Slip Events from Rate and State Friction?

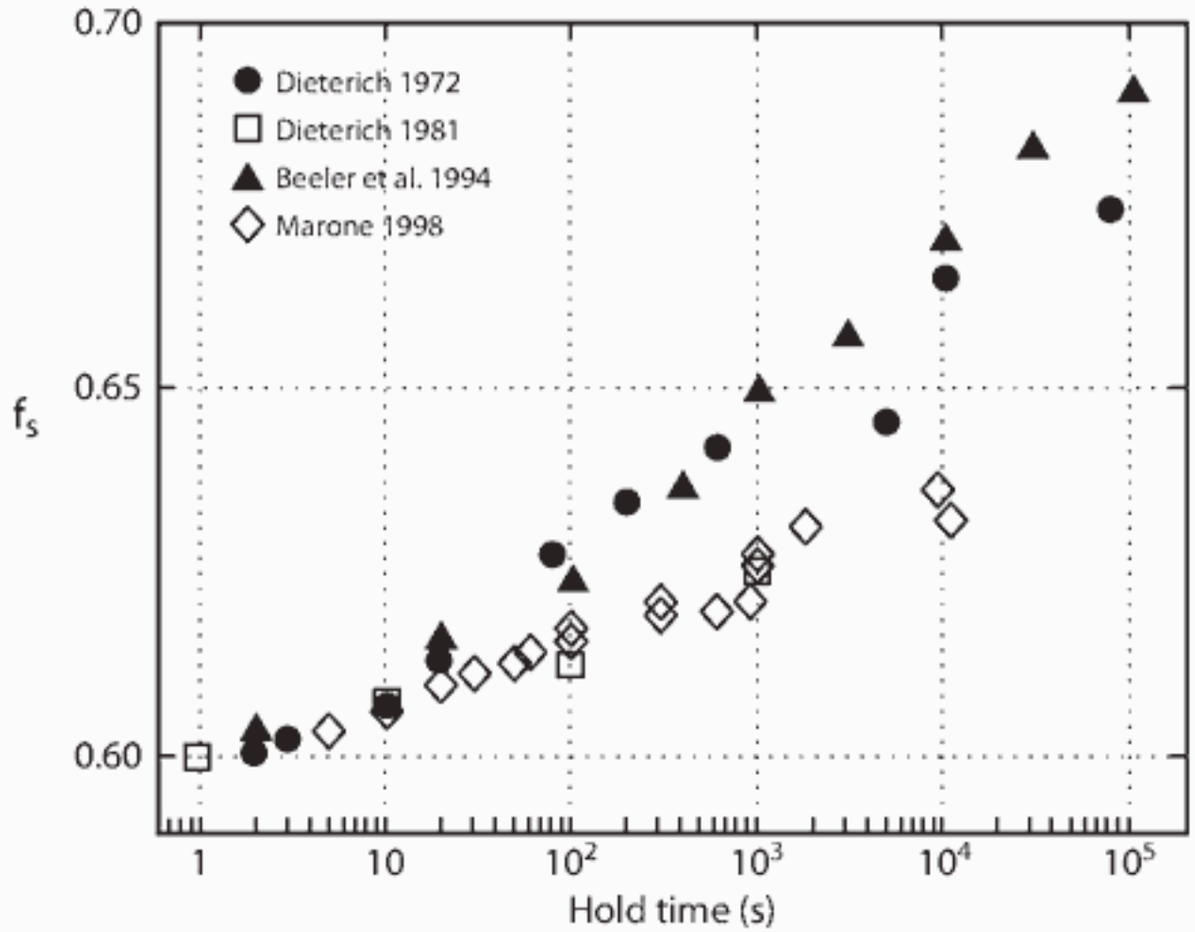

Figure 11.4. Variation in static friction coefficient f_s with hold time. Initially bare rock surfaces (solid symbols) and fault gouge (open symbols). The data have been offset to a friction coefficient of 0.6 at 1 second so that they represent relative changes in friction. After Marone (1998).

See Segall, "Earthquake and Volcano Deformation" Chapter 11.1-11.3

Slow Slip Events from Rate and State Friction?

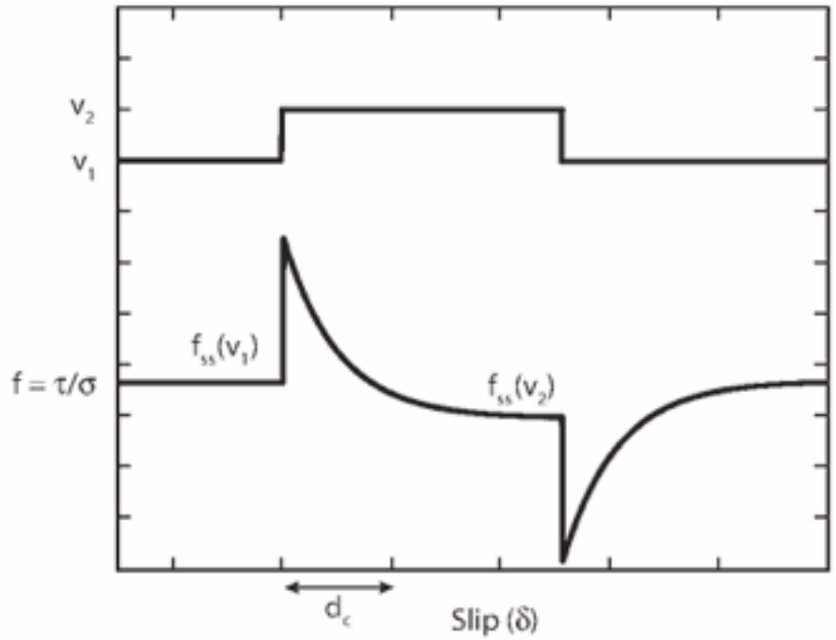

Figure 11.5. Schematic illustration of a velocity stepping test. The load point velocity (upper curve) is suddenly changed from v_1 to v_2. The frictional resistance shows an instantaneous increase followed by a decay to a lower value. The final value may be less than the initial friction, termed *steady-state velocity weakening*, as in this example, or greater than the initial friction, termed *steady-state velocity strengthening*.

the idea

rocks actually do this

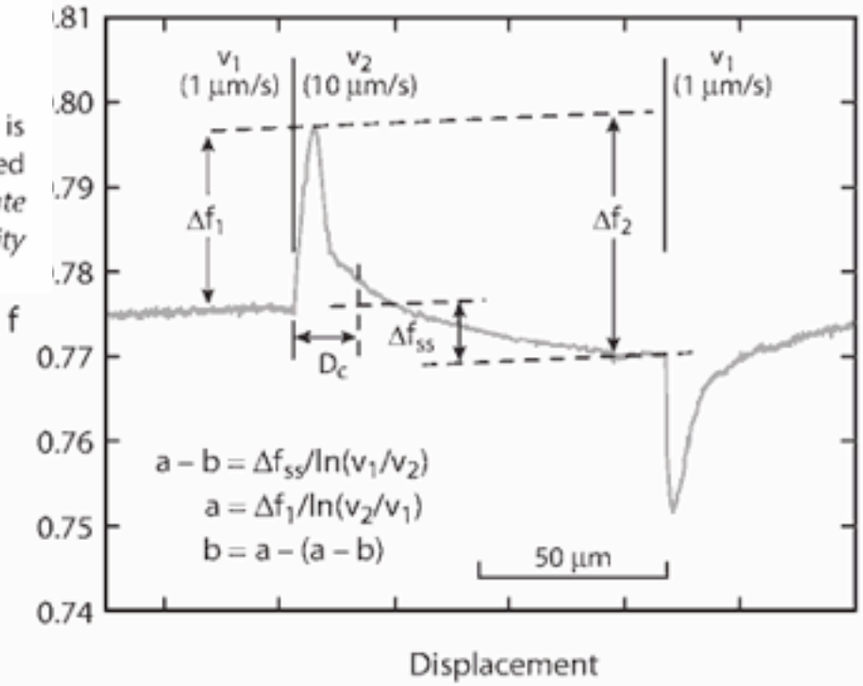

Figure 11.6. Laboratory results for a velocity stepping test, showing transient and steady-state changes in friction. The rapid response to the velocity step Δf_1 gives the constitutive parameter a. The subsequent evolution of the friction coefficient with slip Δf_2 yields the parameter b, so the steady-state change Δf_{ss} is given by $a - b$. This sample exhibits steady-state velocity weakening. Experiment at 150 mpa normal stress. After Kilgore et al. (1993).

See Segall, "Earthquake and Volcano Deformation" Chapter 11.1-11.3

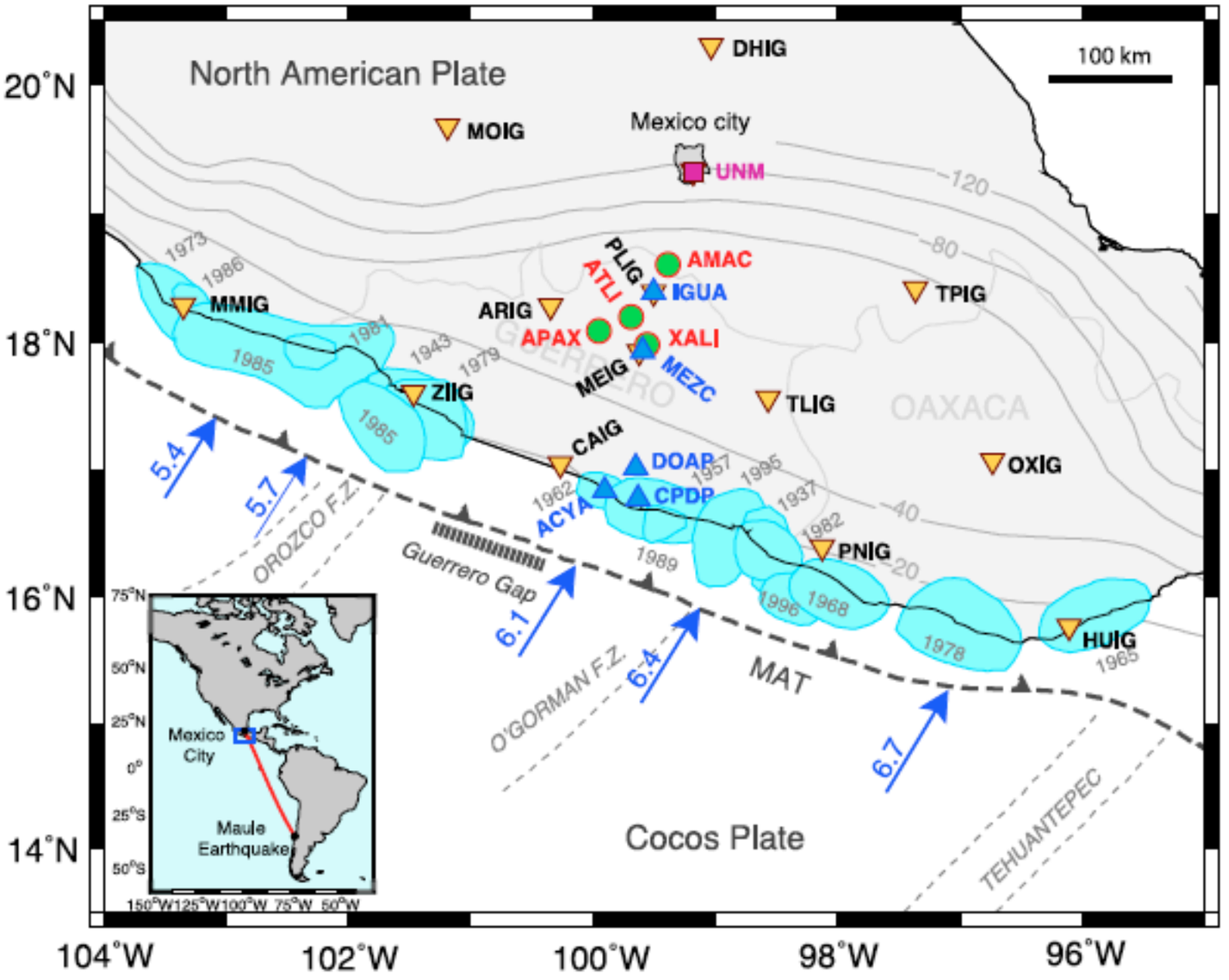

Figure 1. Seismotectonic map of Guerrero, Mexico [after *Kostoglodov et al.*, 2003]. Inverse yellow triangles with black contours indicate the STS2 3 components stations from the Servicio Sismológico Nacional (SSN) of Mexico. The names of these stations are indicated in black. The green dots with red contours indicate the G-GAP miniarrays (1 CMG40 3 components sensor and 6 vertical short period sensors). The G-GAP array's names are indicated in red. The purple square is the STS1 broadband UNM Geoscope station in Mexico City. The blue triangles are the GPS stations used in this study (the names are in blue). The blue arrows indicate the direction and velocity in cm/yr of the PVEL relative plate motion between the Cocos and North American Plate [*DeMets et al.*, 2010]. Little blue patches represent the major earthquakes rupture zones. Thin gray lines show the isodepth contours of the subducted oceanic slab [after *Pardo and Suarez*, 1995]. The insert presents the great circle path between the epicenter of Maule earthquake and UNM station in Mexico City (red line). The blue square indicates the location of the main map.

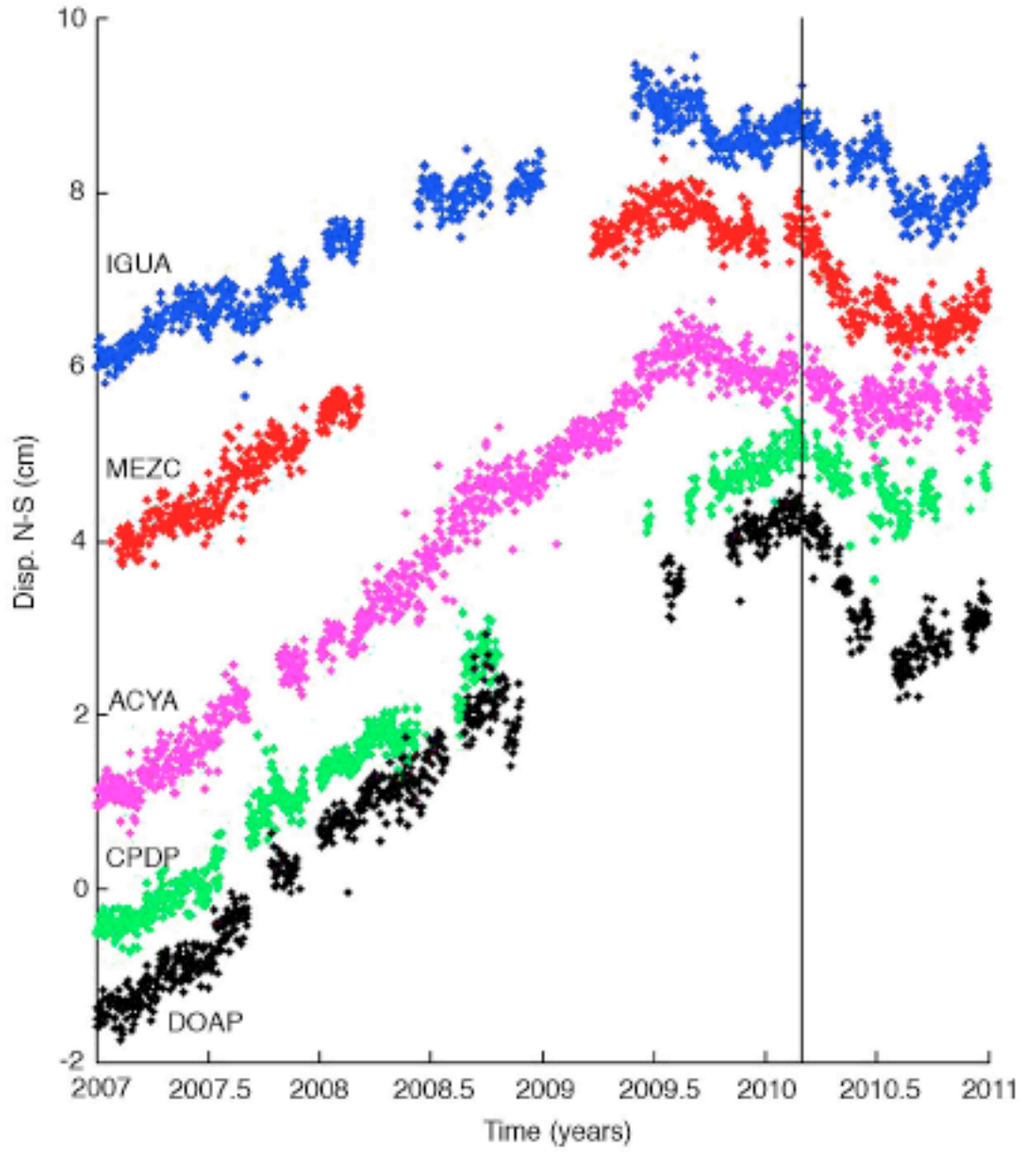

Figure 7. GPS North-south component time series between 2007 and 2011 for various stations in central and eastern Guerrero: IGUA (blue), MEZC (red), ACYA (purple), CPDP (green) and DOAP (black). Black line stands for the Chile earthquake occurrence.

Nankai Trough, Japan

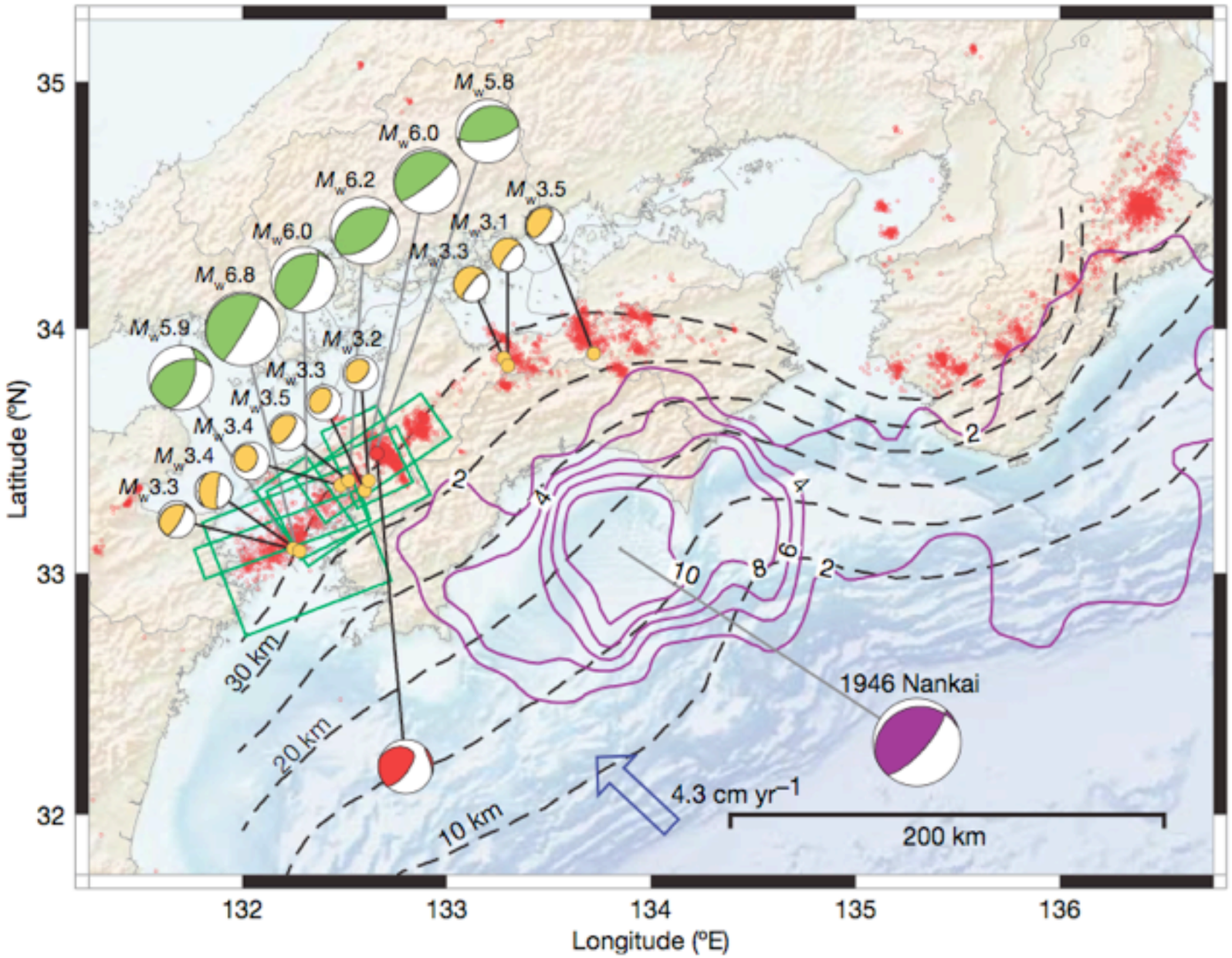

Figure 1 | Various types of earthquakes and their mechanisms along the Nankai trough, western Japan. Red dots represent LFE locations determined by the Japan Meteorological Agency[2]. Red and orange 'beach balls' show the mechanism of LFEs[15] and VLFs[3], respectively. Green rectangles and beach balls show fault slip models of SSE[4]. Purple contours and the purple beach ball show the slip distribution[31] (in metres) and focal mechanism[16] of the 1946 Nankai earthquake ($M_w = 8$). The top of the Philippine Sea plate is shown by dashed contours[12]. The blue arrow represents the direction of relative plate motion in this area[17].

Ide et al., 2007, *Nature*

A Bestiary of Slow Earthquakes

Recently, a series of unusual earthquake phenomena have been discovered, including deep episodic tremor[1], low-frequency earthquakes[2], very-low-frequency earthquakes[3], slow slip events[4] and silent earthquakes[5–9]. Each of these has been demonstrated to arise from shear slip, just as do regular earthquakes, but with longer characteristic durations and radiating much less seismic energy. Here we show that these slow events follow a simple, unified scaling relationship that clearly differentiates their behaviour from that of regular earthquakes. We find that their seismic moment is proportional to the characteristic duration and their moment rate function is constant, with a spectral high-frequency decay of f^{-1}. This scaling and spectral behaviour demonstrates that they can be thought of as different manifestations of the same phenomena and that they comprise a new earthquake category. The observed scale dependence of rupture velocity for these events can be explained by either a constant low-stress drop model or a diffusional constant-slip model. This new scaling law unifies a diverse class of slow seismic events and may lead to a better understanding of the plate subduction process and large earthquake generation.

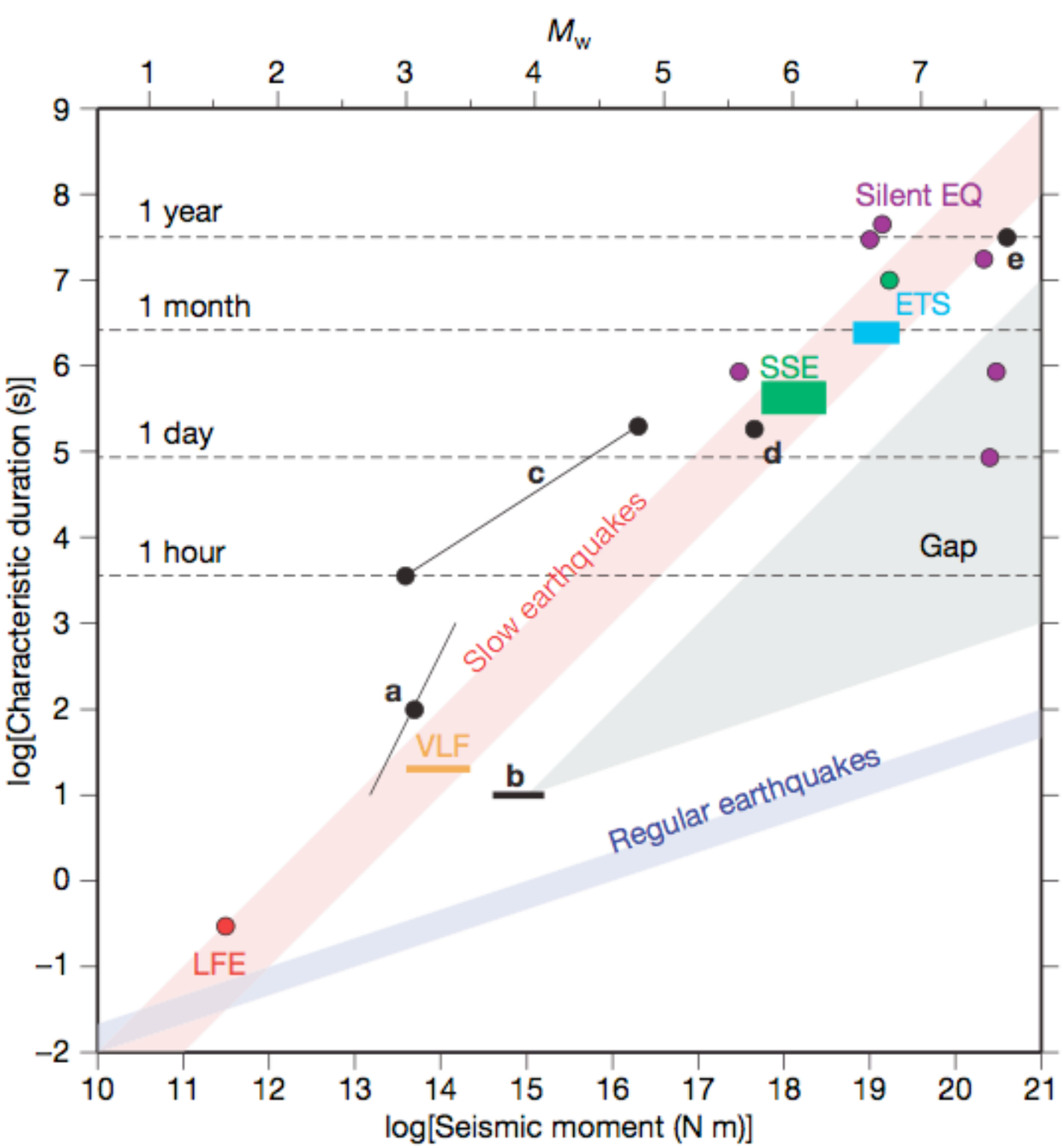

Figure 2 | Comparison between seismic moment and the characteristic duration of various slow earthquakes in Table 1. LFE (red), VLF (orange), and SSE (green) occur in the Nankai trough while ETS (light blue) occur in the Cascadia subduction zone. These follow a scaling relation of $M_0 \propto t$, for slow earthquakes. Purple circles are silent earthquakes. Black symbols are slow events listed in the bottom half of Table 1. **a**, Slow slip in Italy[23,24], representing a typical event (circle) and proposed scaling (line). **b**, VLF earthquakes in the accretionary prism of the Nankai trough[26]. **c**, Slow slip

Ide et al., 2007, *Nature*

Slow earthquakes triggered by Typhoons?

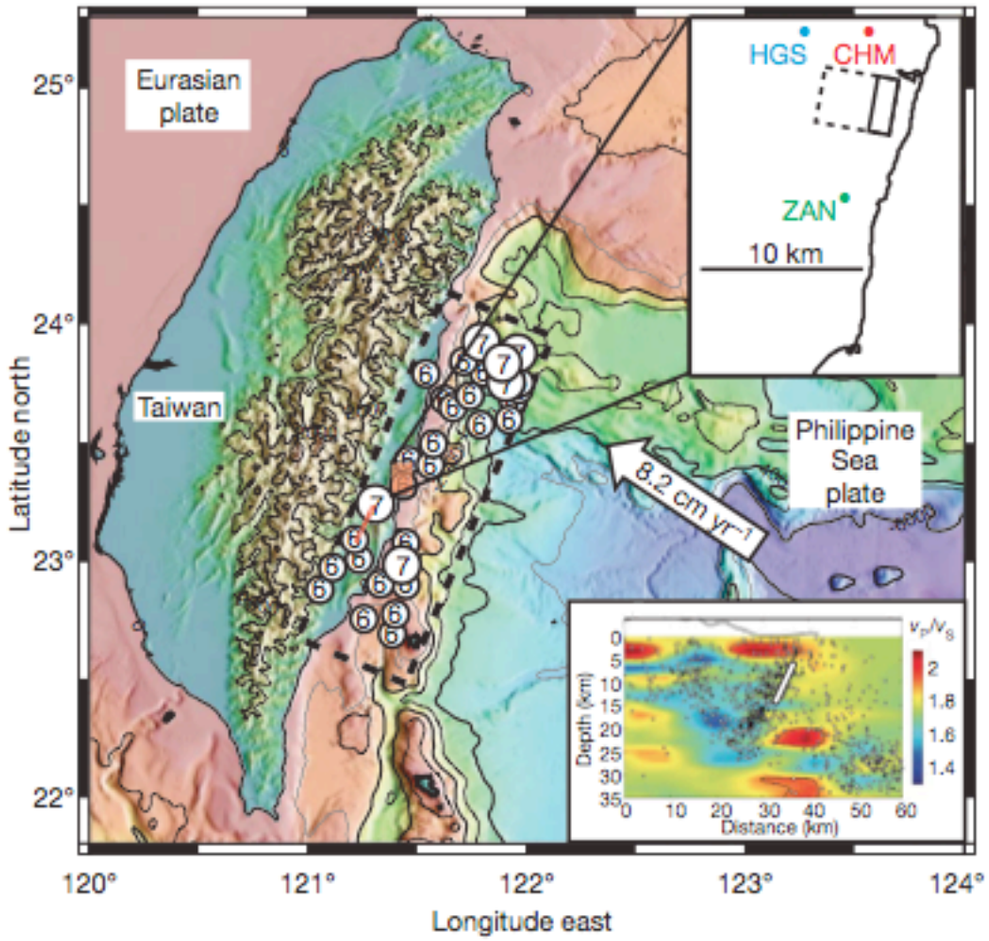

Figure 1 | Topographic map of Taiwan showing collision with Philippine Sea plate. Earthquakes shown (in dashed rectangular area) are all since 1900 and have $M_L > 6$. Of these only one (in 1972) could possibly relieve slip on our model source. Red thick line indicates a creeping zone. Upper inset: study area, showing site locations and plan view of model rupture surface for slow earthquake. Lower inset: seismic section for a profile close to the sites, indicative of a west-dipping normal fault. White rectangle shows location of model rupture. v_P, P-wave velocity; v_S, S-wave velocity.

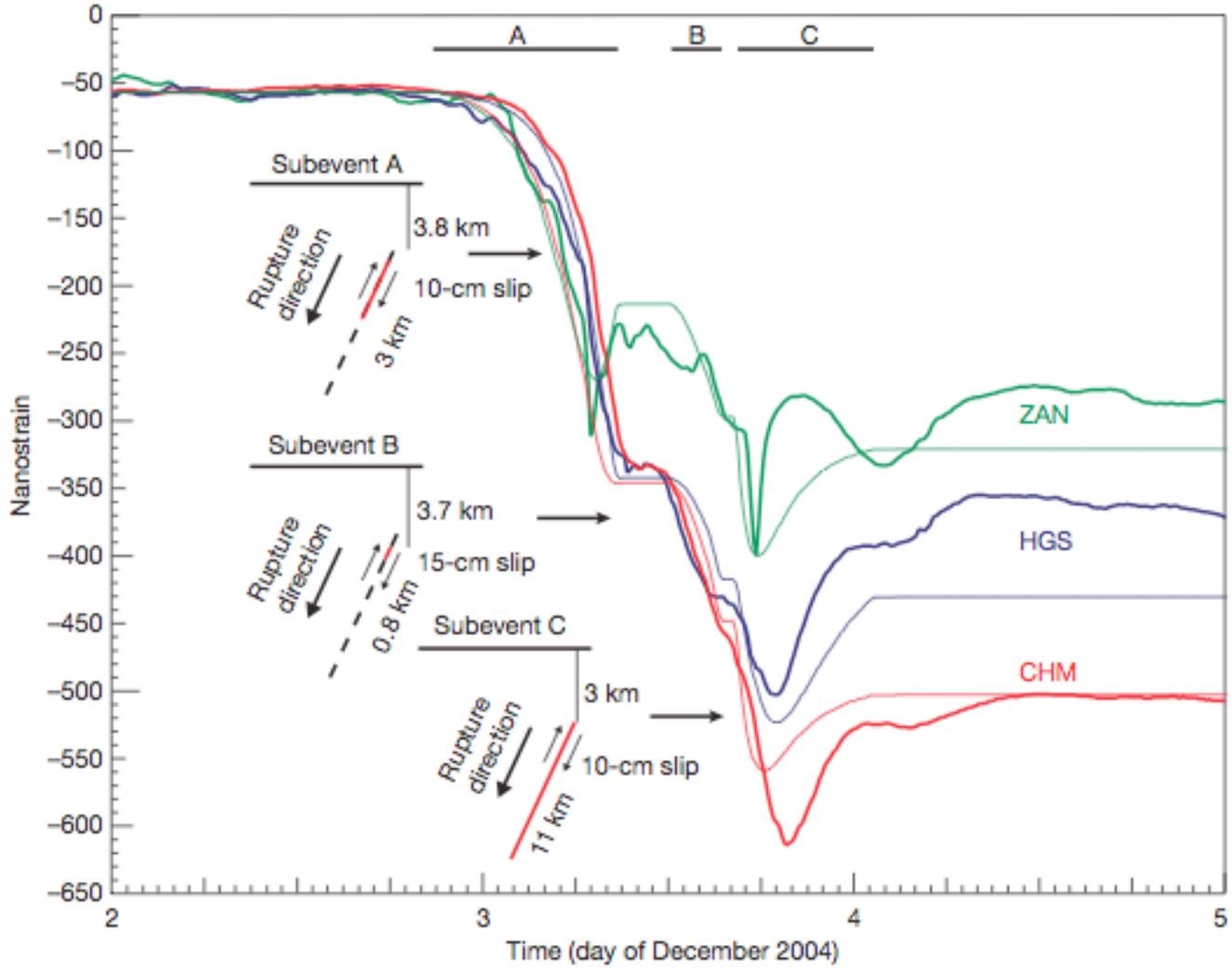

Liu et al., 2009, *Nature*
see class page for .pdf

Figure 3 | Data for the same event as in Fig. 2 but after removal of tidal frequencies and atmospheric pressure-induced changes. We divide the event into three stages, indicated by bars A, B and C. Model vertical sections are shown on the left; see Fig. 1 for fault location. Fault lengths are all 3 km. Reverse slip propagates down dip to different depths for deeper slip results in a nodal line sweeping past the sites producing the reversals in strain. All slips are constant alo dip. This provides a good fit to the data.

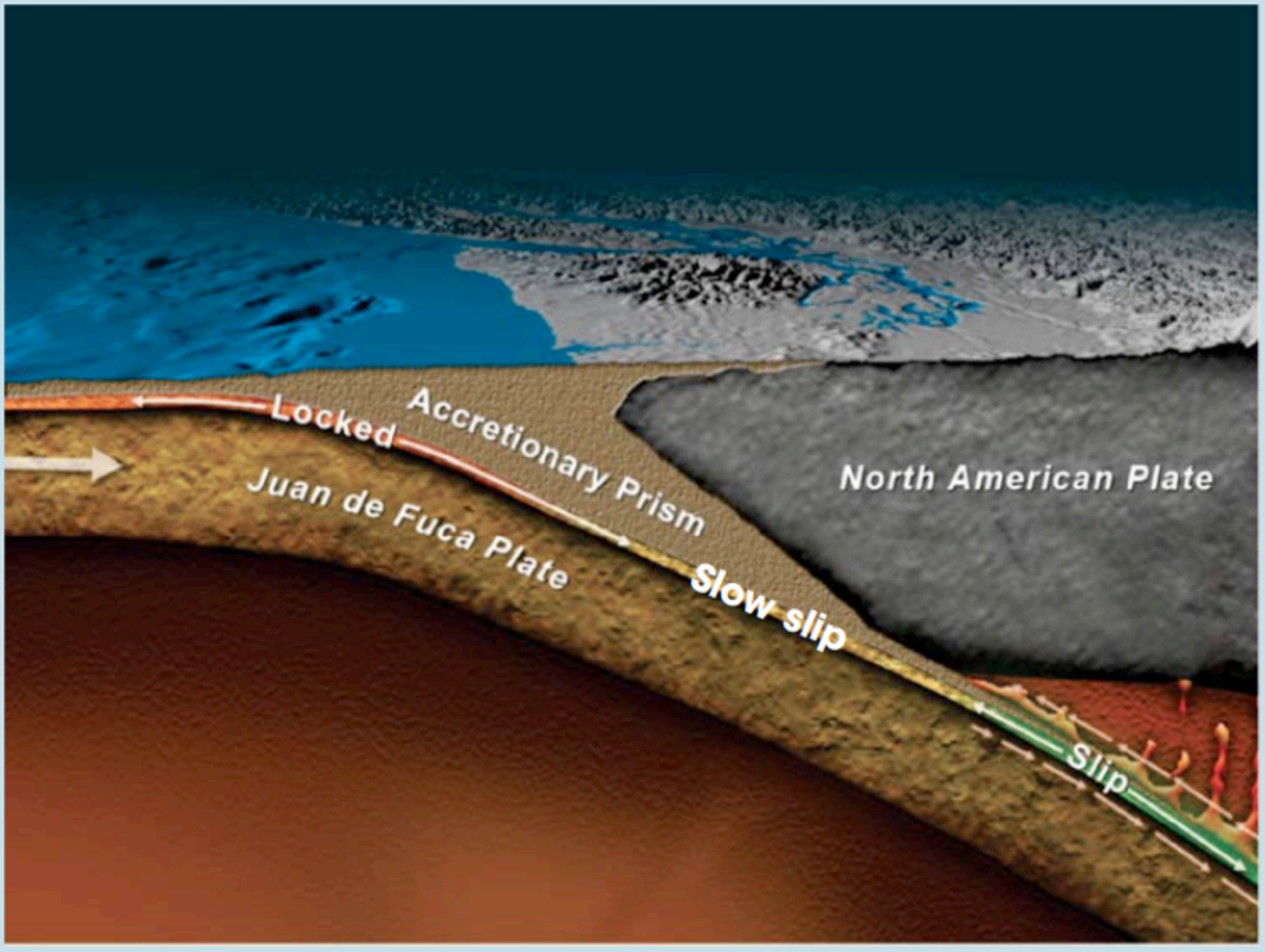

Figure 1. Slow slip appears most prominently in subduction zones, on the plate boundary between the shallow, locked section and the deeper, freely slipping section. The illustration shows an east–west cross section beneath Seattle, Washington, and Vancouver, British Columbia, Canada, in the Cascadia subduction zone. The Juan de Fuca Plate is pushed under the North American Plate as the two plates move together. Marine sediments scraped off the subducting plate build up in the accretionary prism.

Vidale and Houston, 2012, *Physics Today*

Slow slip events

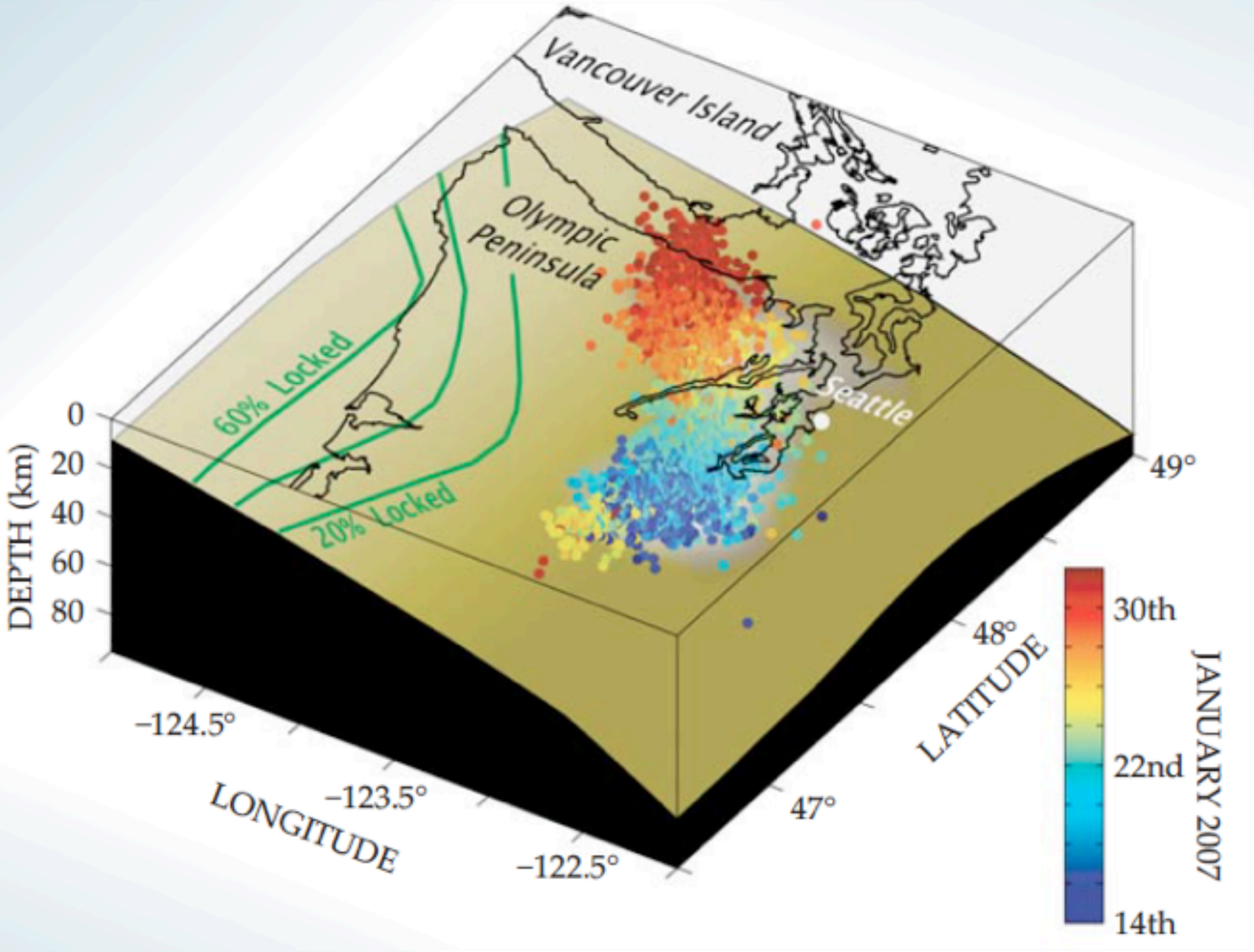

Figure 4. Evolution of a single slow-slip episode in the Cascadia subduction zone. The episode started with the deep blue dots near the southern end, spread bilaterally for a few days, and continued to the north for the rest of the 2 weeks shown. (Courtesy of Aaron Wech.)

Vidale and Houston, 2012, *Physics Today*